

Article

Optimizing Inoculation Conditions for a Two-Strain Fermentation of H₂ Production

Hanxiao Ma^{1,*} and Qian Kang²¹ College of Chemistry and Chemical Engineering of Yan'an University, Yard 580, Shrine Road, Baota District, Yan'an 716000, China² Department of Basic Science, Tianjin Agricultural University, No. 22, Jinjing Road, Xiqing District, Tianjin 300384, China

* Correspondence: mahanxiaoabc@126.com

How To Cite: Ma, H.; Kang, Q. Optimizing Inoculation Conditions for a Two-Strain Fermentation of H₂ Production. *Journal of Green Energy and Green Chemicals* **2025**, *1*(1), 2.

Received: 27 May 2025

Revised: 6 July 2025

Accepted: 9 July 2025

Published: 11 July 2025

Abstract: In order to improve the H₂-production of *Bacillus cereus* (*B. cereus*) and *Brevundimonas naejangsanensis* (*B. naejangsanensis*) by dark fermentation and provide the preferred inoculation conditions for better understanding the process of a co-culture fermentative hydrogen production by both strains, initial inoculation conditions for the single fermentation of both strains were optimized. Results showed that the preferred initial inoculation conditions are 15 h (4.62×10^6 CFU/mL) and 96 h (5.00×10^7 CFU/mL). At the end of fermentation, the highest H₂ yield is 1.93 mol H₂/mol glucose consumed and 1.98 mol H₂/mol glucose consumed, respectively. The corresponding substrate consumption rates are 62.64% and 53.25%. Results also showed that inoculated seed liquid in the early stage of the deceleration growth phase has the capacity of both the effective utilization of starch and production of hydrogen for *B. cereus*, and that in the late stage of the deceleration growth phase has the similar effect for *B. naejangsanensis*. The time required to decompose starch to soluble sugar of *B. cereus* is faster 24 h than that of *B. naejangsanensis*. When metabolic pathway shifted to produce lactic and propionic acid, hydrogen production decreased, elevated acetic and butyric acid concentrations correlated with higher hydrogen production. Butyric acid-type fermentation is dominating during the fermentation process of both strains. *B. cereus* demonstrated superior performance for starch-based hydrogen production.

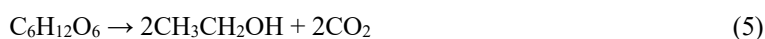
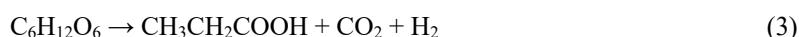
Keywords: biohydrogen production; *Bacillus cereus*; *Brevundimonas naejangsanensis*; initial inoculation conditions

1. Introduction

Dark fermentation is a biological decomposition process reported to be one of the most promising approaches for the treatment of organic wastes. It is also the process commonly used in sustainable bioenergy production [1,2]. As a kind of green bioenergy, hydrogen can be produced by dark fermentation under mild reaction conditions with inexpensive and abundant substrates, such as biomass, biowaste and wastewater [2,3]. Microorganisms utilize these substrates to produce biohydrogen in anaerobic fermentation conditions. Besides the H₂ production pathway (formate H₂ lyase (PFL) pathway and pyruvate: ferredoxin oxidoreductase (PFOR) pathway), H₂ yield also depends on the end-products of the fermentation pathway [4]. For dark fermentation, if acetic acid is the fermentation end-product (Equation (1)), the maximum stoichiometric conversion is 4 mol H₂/mol glucose. If butyric acid is the fermentation end-product (Equation (2)), maximum stoichiometric conversion is only 2 mol H₂/mol glucose due to the associated propionate and the reduced end-products such as alcohols and lactic acid [4].



If propionic acid is produced, H₂ yield are lower (1 mol H₂/mol glucose) (Equation (3)), or H₂ is consumed (in *Propionibacterium*) (Equation (4)), ethanol, propanol, and lactic acid are characteristic of a zero-H₂ pathway [5,6].



In the fermentation process, many factors influence H₂ production, such as temperature, pH, and initial inoculation conditions [7–9]. Initial inoculation conditions (inoculum amount and inoculum age) have been thought to be one of the main influence factors for fermentative H₂ production. Generally speaking, inoculum amount is determined by the bacterial growth and reproduction rates in the fermenter. A larger inoculum amount shortens the time to peak biomass, accelerating product synthesis. Due to the presence of abundant extracellular hydrolytic enzymes in high-concentration seed liquid-which enhance substrate utilization- the entire reactor is rapidly dominated by reproducing strains. However, high cell density may self-limit further growth due to resource competition. Conversely, excessive inoculum transfers a large amount of metabolites from the seed culture into the fermenter, potentially triggering rapid proliferation of bacteria and increasing medium viscosity, both of which impair product synthesis [10]. A low inoculum amount prolongs cultivation time and reduces product yield. Studies on the effect of inoculum size such as initial cell concentration (cells/mL), inoculum amount (%) and inoculation ratio (v/v) on H₂ production are summarized in Table 1. From Table 1, we found that controlling initial inoculum amount has an important influence on H₂ production, as demonstrated in bicellular fermentative systems by Du et al. [11]. Additionally, there is one further point to make, inoculum age is equally critical, ensuring that the seed culture exhibits robust physiological and metabolic activity when transferred into the fermenter.

Table 1. Hydrogen yield under different inoculum condition reported in some literatures.

Inoculums	Substrates	Inoculum Condition	Hydrogen Yield	Refs.
<i>Clostridium butyricum</i> W5	Molasses	9 × 10 ⁴ cells/mL	1.85 mol H ₂ /mol hexose	[12]
<i>Clostridium acetobutylicum</i> YM1	Palm kernel cake hydrolysate	Inoculum size 20%	1575 mL H ₂ /L diluted palm kernel cake hydrolysate	[13]
<i>C. thermocellum</i> + <i>C. thermosgrad</i>	Corn straw	Inoculation ratio 0.25:1 (v/v)	62.0 mL/g cornstalk	[14]
<i>B. cereus</i>	Corn starch	Inoculum amount 10% (v/v)	0.82 mol H ₂ /mol glucose	[15]
<i>B. naejangsanensis</i>	Corn starch	Inoculum amount 10% (v/v)	0.78 mol H ₂ /mol glucose	
<i>B. cereus</i> + <i>B. naejangsanensis</i>	Corn starch	Inoculation ratio 1:1 (v/v)	1.25 mol H ₂ /mol glucose	
<i>B. cereus</i>	Corn starch	Inoculum amount 10% (v/v)	1.03 mol H ₂ /mol glucose	
<i>B. naejangsanensis</i>	Corn starch	Inoculum amount 10% (v/v)	0.99 mol H ₂ /mol glucose	[16]
<i>B. cereus</i> + <i>B. naejangsanensis</i>	Corn starch	Inoculation ratio 1:1 (v/v)	1.36 mol H ₂ /mol glucose	
<i>B. cereus</i>	Corn starch	Inoculum amount 10% (v/v)	0.40 mol H ₂ /mol glucose	
<i>B. naejangsanensis</i>	Corn starch	Inoculum amount 10% (v/v)	0.36 mol H ₂ /mol glucose	[5]
<i>B. cereus</i> + <i>B. naejangsanensis</i>	Corn starch	Inoculation ratio 1:1 (w/w)	1.04 mol H ₂ /mol glucose	
<i>B. cereus</i> + <i>B. naejangsanensis</i>	Corn starch	Inoculation ratio 2:1 (w/w)	1.94 mol H ₂ /mol glucose	[17]
<i>B. cereus</i> + <i>B. naejangsanensis</i>	Cassava starch	Inoculation ratio 1:0.5 (v/v)	1.72 mol H ₂ /mol glucose	[18]

Previous results for the two H₂-producing strains showed in Table 1 indicate low hydrogen yields under the tested inoculum conditions. Furthermore, no studies have explored the effects of initial inoculation conditions (inoculum amount and age) on H₂ production by *B. cereus* and *B. naejangsanensis*.

In order to improve hydrogen yield and production rate of both strains during dark fermentation, it is necessary to study and evaluate the inoculum amount and corresponding inoculum age that will provide a foundation for better understanding subsequent co-culture fermentation process, which will help to elucidate the mechanism of H₂ production of both strains during the co-fermentation process. Therefore, the initial inoculation conditions for the single fermentation of *B. cereus* and *B. naejangsanensis* were investigated in this study.

2. Materials and Methods

2.1. Strains Cultivation

Source of *B. cereus* and *B. naejangsanensis*, composition of seed medium, condition of culture and inoculation of seed liquid are the same as reported before [15]. Glycerol tubes of both strains were stored at -80 °C in freezer of the laboratory.

2.2. Experimental Procedures

2.2.1. Determination of Growth Curve

In order to determine the range of inoculum age of both strains in the following experiments, their growth curves were made. Firstly, glycerol tubes of both strains preserved at -80 °C were thawed and inoculated into a series of 25 mL test tubes contained 5 mL seed liquid with inoculum amount of 0.1% (v/v). After sealed, they were placed in a constant temperature incubator at 37 °C for static culture. OD₆₀₀ of two parallel samples were determined at each set time point. The OD₆₀₀ of both strains measured at different sampling points and the corresponding times were used to define the growth curves of both strains.

2.2.2. Determination of Calibration Curve Correlating OD₆₀₀ to Effective Bacteria Concentration (CFU/mL)

In order to determine the inoculum amounts of both strains under their optimized inoculum ages, their calibration curves between OD₆₀₀ and effective bacteria concentration (CFU/mL) were made. Glycerol tubes of both strains were defrosted after being taken out of the freezer of -80 °C, and then separately inoculated into 500 mL triangular bottles containing 200 mL seed medium at 0.1% (v/v) inoculum amount. After sealed, triangular bottles were placed in a 37 °C constant temperature incubator and cultured until OD₆₀₀ closed to 1.0. After diluted the bacterial suspension of both strains with different volumes of sterile distill water, a series of diluted samples with different bacterial concentration were obtained, the OD₆₀₀ of each diluted sample was measured. And then 0.5 mL of each diluted sample was put into a centrifugal tube with cover and diluted by 10 times gradient with added 4.5 mL of sterile distill water. Based on the measured OD₆₀₀ of each diluted sample of both strains, the dilution gradients of 10⁻³, 10⁻⁴, 10⁻⁵, 10⁻⁶ of each diluted sample were selected to spread on three parallel plates. Coated plates were cultured in a 37 °C constant temperature incubator, colonies of plates for different diluted gradients were counted after cultured a 5 days. Calibration curves relating OD₆₀₀ of different dilutions to viable bacterial concentration (CFU/mL) were established for both strains, with OD₆₀₀ values as the ordinate (y-axis), and effective bacterial concentration (CFU/mL) as the abscissa (x-axis).

2.2.3. Batch Fermentation Process

After being thawed the glycerol tubes, both strains were inoculated in two test tubes with volume of 25 mL containing 5 mL seed liquid at 1% (v/v) inoculum amount, respectively. Then test tubes were sealed and placed in a constant temperature incubator at 37 °C for static culture, activated for 12 h. Next, the activated seed liquid of both strains was inoculated into a series of triangular bottles with volume of 250 mL containing 200 mL seed culture medium at 1% (v/v) inoculum amount, respectively. Then triangular bottles were placed in a 37 °C constant temperature incubator for static culture. Batch fermentation was carried out like reported methods in the literature [15]. For *B. cereus*, according to the growth curve obtained in Section 2.2.1 and the actual growth state of the seed liquid during the culture process, the seed liquid separately cultured at 6 h, 15 h, 48 h, 58 h and 70 h was inoculated into the fermentation medium at 10% (v/v) inoculum amount. The same method was used for *B. naejangsanensis*: the seed liquid of *B. naejangsanensis* separately cultured at 12 h, 60 h and 96 h were inoculated into the fermentation medium at 10% (v/v) inoculum amount. The method of gas collection and measurement was the same as described by Ma et al. [15]. As depicted by Ma et al. [16], a specific structure was designed for fermenter to maintain

anaerobic conditions during fermentation. When hydrogen generation decreased to a great extent, hydrogen fermentation was stopped.

2.3. Analytical Methods

2.3.1. Determination of Some Fermentation Parameters

Methods to determine main parameters—including pH, H₂ content, volatile fatty acids (VFAs), and substrate consumption rate during fermentation—were consistent with the methodology described by Ma et al. [15]. pH was monitored by portable pH probe.

2.3.2. Determination of Soluble Sugar Concentration

After being shaken, 1 mL fermentation broth was transferred into a test tube, and then 1 mL DNS reagent was added. After thorough mixing, the mixture was submerged in boiling water bath for exactly 5 min to develop color, then immediately cooled in cold water to terminate the reaction. Subsequently, the solution was diluted to a final volume of 10 mL with deionized water. The OD₅₄₀ of the diluted solution was determined [19]. According to the calibration curve of absorbance-glucose concentration, the corresponding soluble sugar concentration equivalent in the original 1 mL fermentation broth was calculated.

2.3.3. Determination of Cell Concentration

Uniformly mixed fermentation broth from all groups was collected at appropriate intervals for analyzing cell concentration. Samples for measurement were centrifuged at 500 rpm, and supernatants were used to determine OD₆₀₀ [16].

2.3.4. Calculation of H₂ Production Efficiency

H₂ production efficiency at the end of fermentation was calculated using (Equation (6)):

$$\text{H}_2 \text{ production efficiency} = \frac{\text{Amount of H}_2 \text{ produced (mol)}}{\text{Amount of substrate consumed (mol)}} \quad (6)$$

where the amount of H₂ produced (mol) was obtained by dividing the cumulative hydrogen production (L) at the end of fermentation by the molar volume of gas (22.4 L/mol). The amount of substrate consumed (mol) was calculated from the reducing sugar concentration difference (g/L) multiplied by the culture volume (L), then divided by the molecular weight of glucose (180 g/mol). H₂ production efficiency was defined as mol H₂ per mol substrate consumed.

3. Results and Discussion

3.1. Growth Curve

Growth curves of both strains were obtained (Figure 1). According to reports in the literature [20], *B. cereus* exhibits a five-phase growth process. After a short lag phase of 2 h, the exponential phase begun and lasted 10 h, followed by the deceleration phase until 78 h. The stationary phase persisted until 160 h, after which cells entered the decline phase. From Figure 1, it can also be seen that *B. naejangsanensis* exhibits a four-phase growth process. After a lag phase of 12 h, the exponential phase started and lasted until 96 h, followed by the deceleration phase until 154 h. The stationary phase continued to 154 h onwards. According to the growth curves of both strains, their appropriate inoculum ages could be selected from the exponential and the deceleration phases. More specifically, the ranges of appropriate inoculum ages were determined as 2–78 h and in 12–154 h, respectively. Based on these growth curves, generation times were also calculated as 1.2 h and 34 h, respectively. The calculation formula for generation time was as follows (Equation (7)):

$$G = \frac{t_2 - t_1}{(\lg w_2 - \lg w_1) / \lg 2} \quad (7)$$

in which G (h⁻¹) is the generation time (the time required for cell division); t_1 and t_2 (h) are selected time points during the exponential phase; w_1 and w_2 represent OD₆₀₀ measurements at corresponding time points. Calculation of generation times enables better understanding of strain growth kinetics and facilitates precise control of seed liquid and culture plate incubation time. Specifically, determining the generation times of these new H₂-producing strains contributes significant physiological data to the knowledge base of related field.

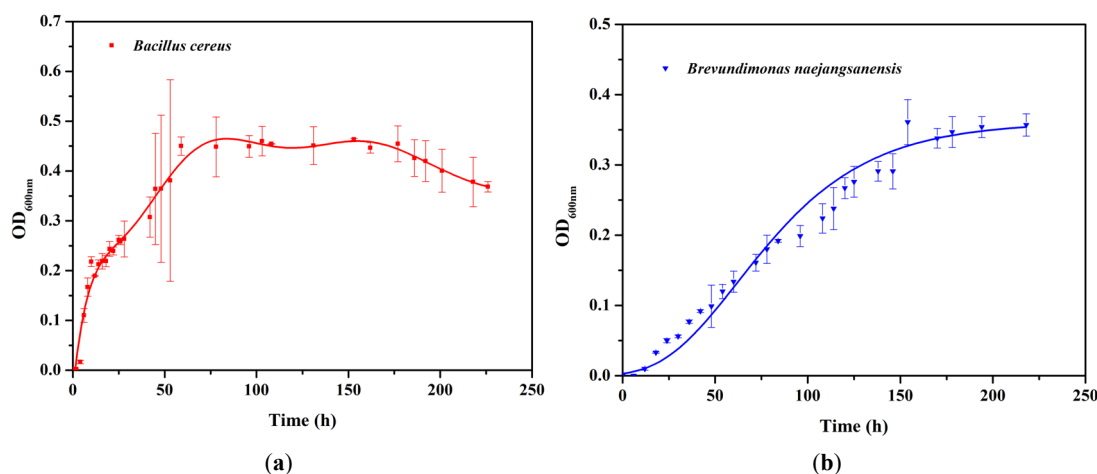


Figure 1. Growth curves of both strains: (a) *B. cereus*; (b) *B. naejangsanensis*.

3.2. Calibration Curve Correlating OD₆₀₀ to Effective Inoculum Concentration (CFU/mL)

Figure 2 shows the calibration curves correlating OD₆₀₀ with the effective inoculum concentration (CFU/mL) for both H₂-producing strains with relative R² values of 0.95 and 0.82. These R² values, exceeding the commonly used acceptability threshold of 0.80, indicate that the calibration curves can provide adequate fitting for predictive purposes within the tested range. The established calibration curves enable the prediction of the effective inoculation concentration (CFU/mL) based on the measured OD₆₀₀ of the corresponding seed liquid at the selected inoculum age.

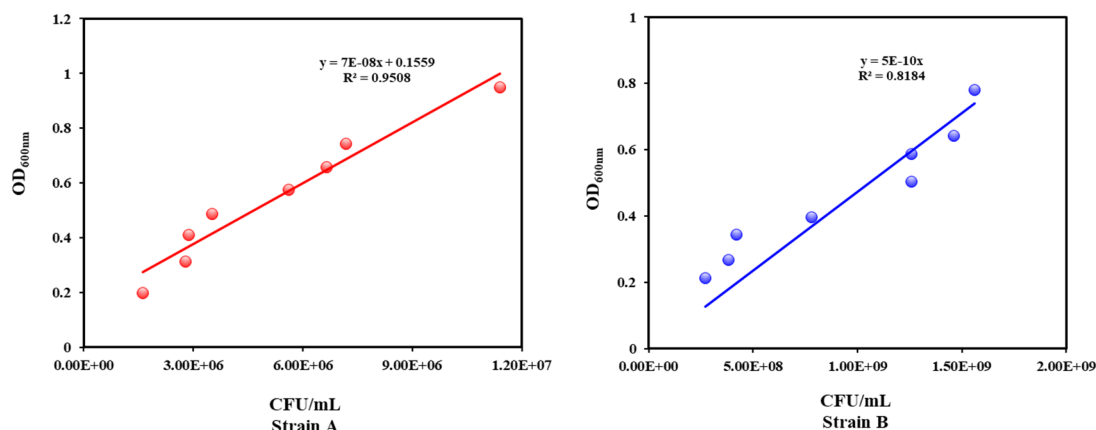


Figure 2. Calibration curves between OD₆₀₀ and effective inoculation concentration (CFU/mL) of both strains.

3.3. Variation of the Main Process Parameters during the Fermentation of Both Strains under Different Initial Inoculation Conditions

3.3.1. Biomass

Figure 3 shows the cell growth profile of both strains during the fermentation process under different initial inoculation conditions. From Figure 3a, it is evident that for *B. cereus*, after a short lag phase, an early onset of the exponential phase occurred likely due to sufficient carbon sources and nutrients in the fermentation medium. The deceleration phase began after 24 h, followed by the stationary phase, which lasted from 108 h onwards. For the group with an inoculum age of 6 h, strains grew slowly at the initial stage, and cell concentration was lower than that of other groups. In addition, cell activity was inhibited in advance for the group with an inoculum age of 70 h, hydrogen production also ceased (Figure 4a). This illustrates that too young or too old inoculum ages have an adverse effect on the growth of *B. cereus* during the fermentation process. However, by 180 h, the highest concentration shifted to the culture with an inoculum age of 15 h. Although the cell concentration peaked for the inoculum age of 58 h between 132 h and 156 h, this group exhibited slower growth during the deceleration phase compared to cultures with inoculum ages of 15 h and 48 h. This indicates that the optimal inoculum ages for *B. cereus* were between 15 and 48 h.

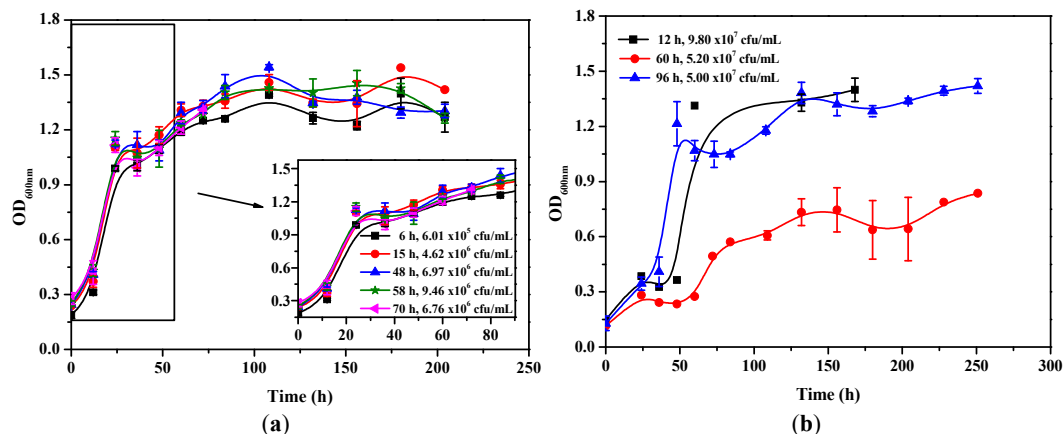


Figure 3. Time course of OD₆₀₀ for *B. cereus* (a) and *B. naejangsansensis* (b) under different inoculation conditions.

From Figure 3b, the cell growth profile of *B. naejangsansensis* differs significantly from that of *B. cereus*. In groups with inoculum ages of 12 h and 60 h, cells exhibited growth arrest after a brief exponential phase before resuming proliferation. For the group with inoculum age of 96 h, cells entered a short lag phase followed by an exponential phase lasting until 48 h, then progressed to the deceleration phase. The stationary phase began from around 156 h onward. Growth arrest in the 12 h and 60 h groups likely resulted from lactic acid accumulation (Figure 9b), as starch decomposition in *B. naejangsansensis* generates glucose for both biomass synthesis and pyruvate-derived lactic acid production [21]. This metabolic shift inhibits growth when lactate pathways dominate. Notably, the inoculum group of 96 h achieved the fastest growth (OD₆₀₀ reached 1.214 at 48 h), indicating maximal metabolic activity in this cohort.

3.3.2. Cumulative Hydrogen Production

Figure 4 depicts the variation of cumulative H₂ production during the fermentation of both strains under different initial inoculation conditions. As described in the literature, the metabolic pathway for H₂ production using glucose includes the pyruvate decarboxylation or the formate cleavage process, all of which occur during exponential growth phase [22,23]. Combined with the results shown in Figure 3, hydrogen generation started at the exponential growth phase with the highest H₂ volume production during the stationary growth phase (Figure 4a,b). For *B. cereus*, high hydrogen generation lasted until 108 h, which was followed by a decrease in hydrogen evolution, indicating the onset of the stationary phase of the cell growth profile.

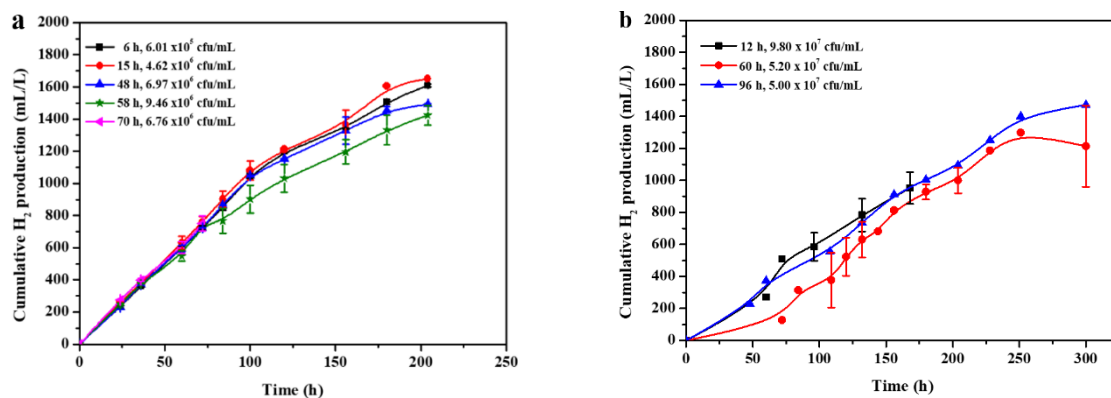


Figure 4. Time course of cumulative H₂ production for *B. cereus* (a) and *B. naejangsansensis* (b) under different inoculation conditions.

For *B. naejangsansensis*, high hydrogen generation lasted until 72 h, which was followed by a decrease in hydrogen evolution, indicating the onset of the stationary phase of the cell growth profile for the group with an inoculum age of 12 h. For the groups with inoculum ages of 60 h and 96 h, high hydrogen generation continued until 156 h, which was followed by a decrease in hydrogen evolution, indicating the onset of the stationary phase of the cell growth profile. A drop in hydrogen production volume could be attributed to a shift in the metabolic pathway to produce lactic acid (shown in Figure 9b). As reported in the literature [24], increased lactic acid production was not conducive to hydrogen production. The reason is that lactic acid formation is coupled with the

oxidation of NADH, leading to a decrease in the availability of NADH for hydrogen production [25]. Another reason for the drop in hydrogen production volume could be the inhibitory effects of VFAs (acetic acid and butyric acid) formed during the hydrogen evolution process by H₂-producing bacteria [16,26]. The maximum cumulative hydrogen production was reached during the stationary phase, and hydrogen production ceased during this phase, as reported in the literature [20]. Combining the results shown in Figures 3 and 4, it can be observed that hydrogen production was coupled with the growth of both strains during the fermentation process.

3.3.3. pH

The initial pH of medium decisively influences the activity of enzymes involved in the metabolic pathway of hydrogen generation by hydrogen-producing microorganisms in the dark fermentation process [20]. Figure 5 shows the variation in pH during the fermentation for both strains under different initial inoculum conditions. As can be observed, except for the group of *B. naejangsanensis* with an inoculum age of 12 h (initial pH 6.1), the initial pH was around 6.3 for both strains. This range (5.0–7.0) falls within the optimal initial pH reported for hydrogen production systems [16]. From Figure 5a, pH of the fermented broth fluctuated dramatically within the first 24–72 h. After 72 h, pH trends became similar for the groups with inoculum ages of 6 h, 15 h and 48 h, ultimately decreasing to approximately 3.95 by the end of fermentation. Furthermore, after 24 h, the pH for the group with the highest inoculum amount (58 h age) decreased to its lowest point (4.16), while the pH for the other groups decreased rapidly from approximately 6.30 to about 4.50. This rapid decline indicates that the initially higher cell concentration in the high-inoculum group led to more vigorous bacterial growth and metabolism within 24 h, accelerating acid production and the pH drop. This low pH subsequently inhibited bacterial activity. Similar phenomena have been reported in the literature [27,28].

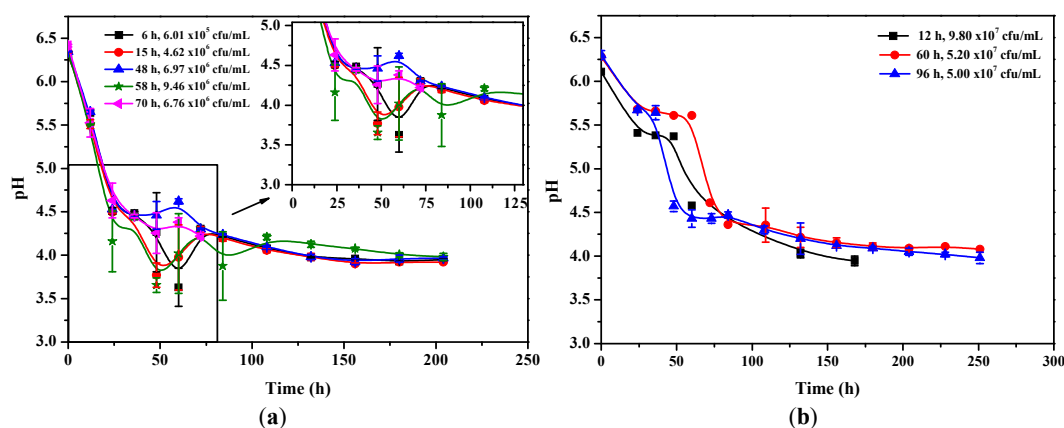


Figure 5. Time course of pH for *B. cereus* (a) and *B. naejangsanensis* (b) under different inoculation conditions.

As can be observed from Figure 5b, pH under different initial inoculation conditions dramatically changed within 24–84 h. After 84 h, pH continually decreased for the group with an inoculum age of 12 h and reached 3.95 by the end of fermentation. For the other two groups, pH trends were similar and decreased to approximately 4.03 by the end of fermentation. The pH fluctuation was probably caused by the vigorous growth and metabolism of bacteria, and the secretion of a large number of organic acids during the fermentation. Additionally, as shown in Figure 5b, pH of the groups with inoculum ages of 12 h and 60 h dropped to 5.41 and 5.68 after 24 h, respectively. Due to the growth of cells and secretion of abundant organic acids in the fermentation, their pH dropped rapidly again at 48 h (12 h inoculum) and 60 h (60 h inoculum) respectively. For the group with an inoculum age of 96 h, pH rapidly dropped to around 4.5 within 48 h, and then declined slowly. Combined with the variation of the cumulative hydrogen production under different inoculum ages shown in Figure 4b, it can be seen that speed of hydrogen production started to increase for the groups with inoculum ages of 12 h and 60 h after 60 h and 72 h, which can be reflected by the change of the line graph's slope. However, the speed of hydrogen production continued to increase for the group with an inoculum age of 96 h from the beginning of fermentation. Due to the increased concentration of lactic acid (Figure 9b), the initiation of hydrogen production for the group with an inoculum age of 60 h lagged behind those of the other two groups. From the change of pH, it can be inferred that metabolic activity of *B. naejangsanensis* was strong in the initial fermentation stage for the group with an inoculum age of 96 h.

3.3.4. Total Reducing Sugar and Soluble Sugar

According to the reported literature [21], we know that the reducing sugar and the soluble sugar are composed of low molecular-weight oligosaccharides, maltose and glucose. It should be pointed out that starch in the samples was collected at appropriate intervals is hydrolyzed to glucose by dilute hydrochloric acid to determine total reducing sugar concentration, while unhydrolyzed samples are used to determine soluble sugar concentration.

Figure 6 showed the change in the concentration of total reducing sugar and soluble sugar during the fermentation of both strains under different initial inoculation conditions. From Figure 6a,b, it can be seen that the initial concentration of total reducing sugar for both strains under different initial inoculation conditions was about 11.08 g/L and 10.82 g/L, respectively. At the end of fermentation, it was about 4.32 g/L and 5.13 g/L, respectively. As observed in Figure 6a, the concentration of total reducing sugar during the fermentation process showed a trend of rapid decline, but the utilization of reducing sugar varied among groups with different inoculum conditions. Compared with other groups, the consumption of total reducing sugar was the slowest in the initial fermentation stage for the group with an inoculum age of 6 h. However, with the growth and reproduction of *B. cereus*, the consumption rate of total reducing sugar increased for this group, and the concentration decreased to 4.233 g/L by the end of fermentation. Moreover, the consumption rate was the fastest for the group with an inoculum age of 48 h during the first 156 h. However, the highest consumption rate after 156 h was observed in the group with an inoculum age of 15 h, and the concentration reached 4.097 g/L by the end of fermentation. This indicated that cell activity was strongest in the group with an inoculum age of 15 h, resulting in greater robustness against the drastic changes in fermentation conditions caused by accumulated metabolites. Compared with the two groups inoculated during the late deceleration phase of growth (58 h and 70 h), substrates were more thoroughly consumed by the groups with inoculum ages of 6 h, 15 h and 48 h during fermentation, due to their strong cell activity. This indicated that inoculating seeds during the exponential phase and early deceleration phase of growth favored to the effective utilization of substrates for fermentative hydrogen production by *B. cereus*.

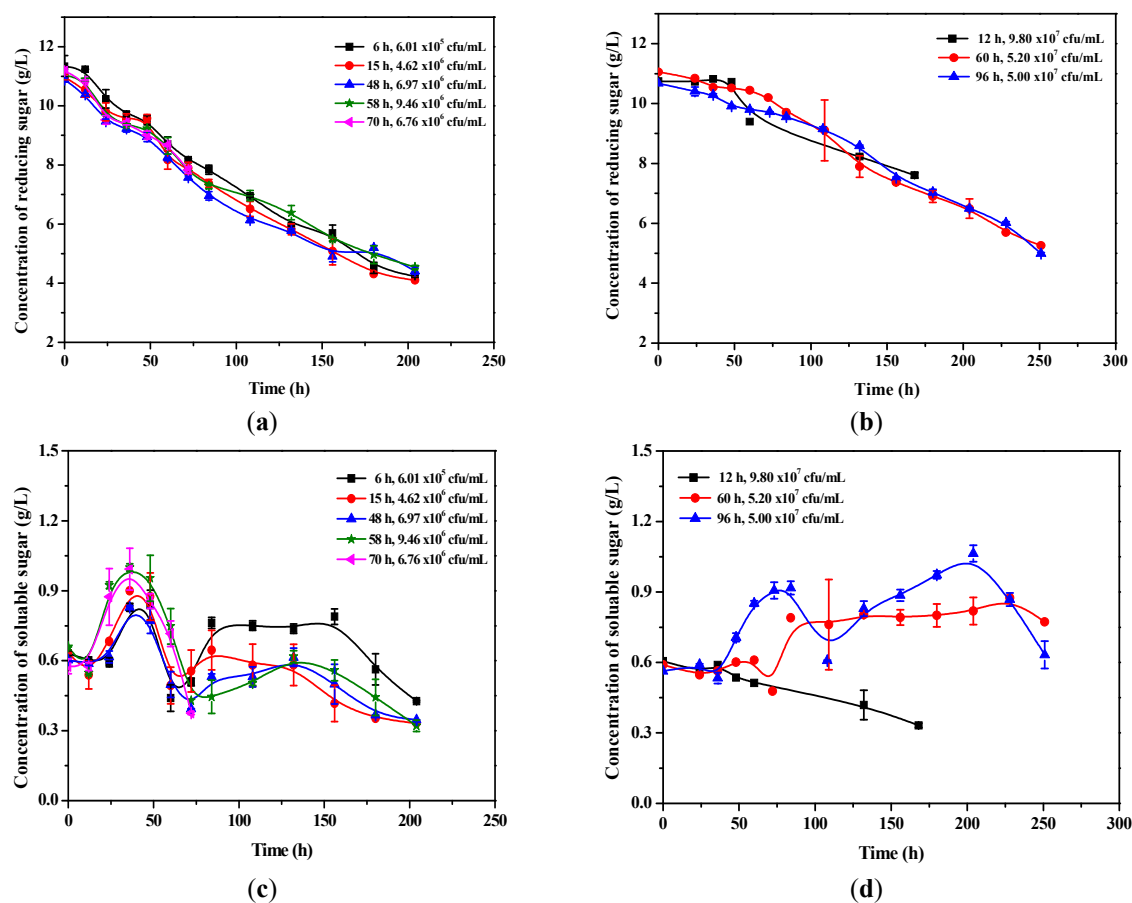


Figure 6. Time course of total reducing sugar and soluble sugar for *B. cereus* (a,b) and *B. naejangsensis* (c,d) under different inoculation conditions.

As shown in Figure 6b, for *B. naejangsensis*, the concentration of total reducing sugar during fermentation under different initial inoculation conditions showed a decreasing trend. It can be observed that for the groups with

inoculum ages of 12 h and 60 h, reducing sugar was barely consumed and changed slowly within 48 h, after which its consumption rate increased. Compared with the other two groups, the group with an inoculum age of 96 h showed the fastest consumption rate of reducing sugar during the first 48 h, with an average value of 0.016 g/L/h in this phase. Combining the results shown in Figures 3b and 5b, it can be inferred that the consumption rate of total reducing sugar was closely associated with the growth state of *B. naejangsanensis* and the pH of the fermentation medium. According to this analysis, when inoculating seed liquid in the early exponential phase of growth, *B. naejangsanensis* needed more time to adapt to the fermentative environment to utilize substrates sufficiently. The consumption rate of reducing sugar was the fastest for the group with an inoculum age of 96 h, indicating that seed liquid in the late exponential phase of growth was more conducive to rapid substrate utilization by *B. naejangsanensis*.

The variation of soluble sugar concentration during fermentation reflects microbial starch-degrading capacity. As shown in Figure 6c,d, *B. cereus* demonstrated faster starch-to-glucose conversion than *B. naejangsanensis*, reaching peak sugar concentration at 36 h across all groups. In contrast, *B. naejangsanensis* peaked at 60 h (60 h inoculum) and 84 h (96 h inoculum). Combining with the results shown in Figure 3b, due to rapid cell growth, the 12 h inoculum group of *B. cereus* exhibited continuous soluble sugar depletion. The group with an inoculum age of 58 h (9.46×10^6 CFU/mL) showed the highest initial soluble sugar accumulation (Figure 6c), followed by rapid metabolic consumption. Notably, slow growth of the 6 h inoculum group after 72 h (Figure 3a) influenced the sugar utilization, leading to residual soluble sugar accumulation. The group with an inoculum age of 15 h initiated sugar consumption after 84 h—the earliest among all groups—confirming its superior metabolic activity. These findings demonstrate that early deceleration-phase inoculation is beneficial to the utilization of soluble sugar in *B. cereus* fermentation.

According to the reported results [21], *B. naejangsanensis* mainly used glucoamylase to act on the reducing ends of starch or oligosaccharides and produced glucose. Combining the results shown in Figure 6d with the biomass change of *B. naejangsanensis*, it was evident that soluble sugar utilization was closely related to its growth state. For the group with an inoculum age of 12 h, due to rapid cell growth, soluble sugar was continuously consumed during fermentation. For the group with an inoculum age of 60 h, soluble sugar concentration slightly increased within 60 h. It reached the lowest level at 72 h corresponding to bacterial growth and metabolism, then increased slightly to near stability. This likely resulted from a dynamic balance between starch decomposition into soluble sugar and its consumption by *B. naejangsanensis* from 84 h to 228 h. Adaptation to the changing environment slowed growth and metabolic rates during this stage. Soluble sugar concentration fluctuated most significantly for the group with an inoculum age of 96 h. It was relatively high at 84 h and 204 h. At these points, the growth rate increased (Figure 3b), leading to rapid subsequent soluble sugar consumption. This group also exhibited the fastest soluble sugar consumption rate, indicating stronger seed activity compared to the other two groups. Comparison of Figure 6c,d revealed that *B. cereus* decomposed starch into soluble sugar approximately 24 h faster than *B. naejangsanensis*. Additionally, peptone in the seed medium contained reducing sugar such as aminosaccharide, which explains why soluble sugar concentration did not start from zero in Figure 6c,d.

3.3.5. H₂ Content

Figure 7 shows the time course of H₂ content for both strains during fermentation under different initial inoculation conditions. As observed in Figure 7a, all groups reached nearly identical peak H₂ content (approximately 60%), indicating that the activation of key enzyme activity in *B. cereus* during the initial fermentative hydrogen production phase was unaffected by inoculation conditions. After 120 h, divergence in H₂ content emerged among groups. The group with an inoculum age of 6 h maintained the highest level. The groups with inoculum ages of 48 h and 58 h exhibited gradual decline. However, it showed unique dynamics for the group with an inoculum age of 15 h, increasing during 120–180 h before declining post-180 h. Combining the results shown in Figures 3a and 4a, it reveals that while the 6 h group demonstrated maximal hydrogen production activity, the 15 h group displayed superior metabolite inhibition resistance and sustained production capability. This correlates with *B. cereus* growth state data in Figure 3a, where the 15 h inoculum maintained better viability than other groups at fermentation termination.

From Figure 7b, it can be seen that the rates at which different groups reached their highest H₂ content varied. This indicates that the activation of key enzyme activity in *B. naejangsanensis* at the beginning of fermentative hydrogen production differed depending on the initial inoculation conditions. In the initial stage, hydrogen production was fastest in the group with an inoculum age of 96 h, which reached its peak H₂ content (62.76%) in the shortest time (60 h). The groups with inoculum ages of 12 h and 60 h reached to their peak H₂ content (60.20% and 58.52%, respectively) at 72 h and 84 h. Compared to the other two groups, the group with an inoculum age of 96 h achieved the highest H₂ content. The changes in H₂ content followed similar patterns in the subsequent fermentation process for all three groups. However, hydrogen production ceased in the group with an inoculum

age of 12 h, while the H₂ content in the other two groups decreased. Notably, the change in H₂ content was relatively small for the group with an inoculum age of 96 h after 60 h. In summary, the bacterial activity was strongest in the group with an inoculum age of 96 h, and hydrogen production commenced most rapidly in this group.

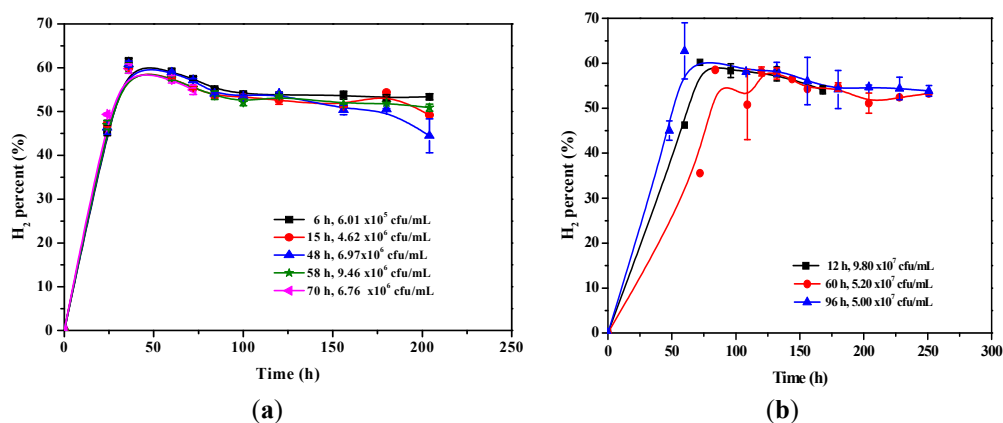


Figure 7. Time course of H₂ content for *B. cereus* (a) and *B. naejangsanensis* (b) under different inoculation conditions.

3.3.6. Variation of Main Extracellular Metabolites

The variations in major extracellular metabolites (including pyruvic acid, lactic acid, propionic acid, formic acid, acetic acid, and butyric acid) were analyzed under different initial inoculation conditions for both strains. As shown in Figures 8–11, the concentrations of pyruvic acid, lactic acid, propionic acid and formic acid were significantly lower than those of acetic acid and butyric acid.

As well-known, pyruvic acid is an important intermediate metabolite in the glycolytic metabolism of microorganisms. Hence, analyzing its concentration changes is significant for better understanding variations in substrate consumption and other main metabolites during the fermentative hydrogen production process for both strains. As Figure 8a shows, within 72 h, the trend in pyruvic acid concentration was similar for groups with inoculum ages of 6 h, 15 h and 48 h, with peak concentrations of 0.059 g/L, 0.045 g/L and 0.047 g/L, respectively. Similarly, for groups with inoculum ages of 58 h and 70 h, peak concentrations were 0.040 g/L and 0.059 g/L, respectively. Thereafter, except for the group with an inoculum age of 70 h, pyruvic acid concentration under other inoculum ages gradually decreased with fluctuations. According to literature [21], pyruvic acid is converted to lactic acid, acetyl-CoA and formic acid during the fermentation process of *B. cereus*. Moreover, considering the glycolysis pathway, under different inoculum ages, changes in pyruvic acid concentration in *B. cereus* are related to changes in reducing sugar and soluble sugar concentrations during fermentation. As shown in Figure 8b, pyruvic acid concentration was relatively high for groups with inoculum ages of 60 h and 96 h, and it reached to the maximum first for the latter group. This indicated that *B. naejangsanensis* exhibited the strongest metabolic activity at an inoculum age of 96 h. Compared to other two groups, pyruvic acid concentration was relatively low for the group with an inoculation age of 12 h. As fermentation progressed, pyruvic acid was gradually utilized by conversion to lactic acid and acetyl-CoA. Comparing the results shown in Figure 8a,b, it can be observed that the rate of starch decomposition to pyruvic acid was faster for *B. cereus* than for *B. naejangsanensis*.

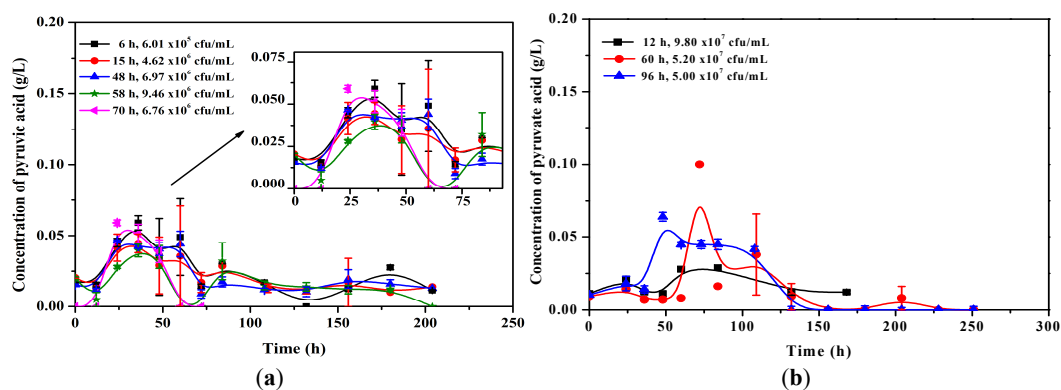


Figure 8. Time course of the concentration of pyruvic acid for *B. cereus* (a) and *B. naejangsanensis* (b) under different inoculation conditions.

Figure 9 shows the variation in the concentration of lactic acid and propionic acid for both strains under different inoculation conditions. It can be observed that their concentration was relatively low in the fermentation broth. From Figure 9a, it is evident that the concentration of lactic acid increased to its maximum at 12 h for *B. cereus*; subsequently, except in the group with an inoculum age of 48 h, it rapidly decreased to zero in other groups. Aside from the group with an inoculum age of 70 h (which stopped producing hydrogen at 72 h), the concentration of lactic acid began to increase again after 100 h in the remaining groups. For groups with inoculum ages of 6 h, 15 h and 48 h, the concentration first increased and then decreased between 100–204 h, reaching peak values of 0.11 g/L, 0.26 g/L and 0.23 g/L, respectively. In contrast, for the group with an inoculum age of 58 h, it increased steadily after 100 h until fermentation ended. Contrary to literature reports [21], lactic acid was detected in the sole fermentation of *B. naejangsansensis* in this study. As shown in Figure 9b, the lactic acid concentration for the group with an inoculum age of 60 h exceeded that of the groups with inoculum ages of 12 h and 96 h, exhibiting an initial increase followed by a decrease, with a peak of 0.363 g/L at 108 h. For the groups with inoculum ages of 12 h and 96 h, the variation showed similar trends, reaching maxima at 48 h and 36 h, respectively, before declining to zero after 60 h. This observation aligns with literature [21], indicating *B. naejangsansensis* can utilize lactic acid as a substrate. Ergal et al. [29] further confirmed lactic acid as a substrate for fermentative hydrogen production. As noted in [29], the initial rise in lactic acid concentration might result from high reactor pressure, as hydrogen pressure increases, NADH regeneration for hydrogen production occurs via lactic acid production mediated by lactate dehydrogenase within microbial cells [30]. Combining with the results shown in Figure 4, it can be known that, an increase in lactic acid during fermentation correlated with reduced hydrogen production rates for both strains. This is consistent with established findings; a metabolic shift toward lactic acid production correlates with diminished or halted hydrogen production [31–33].

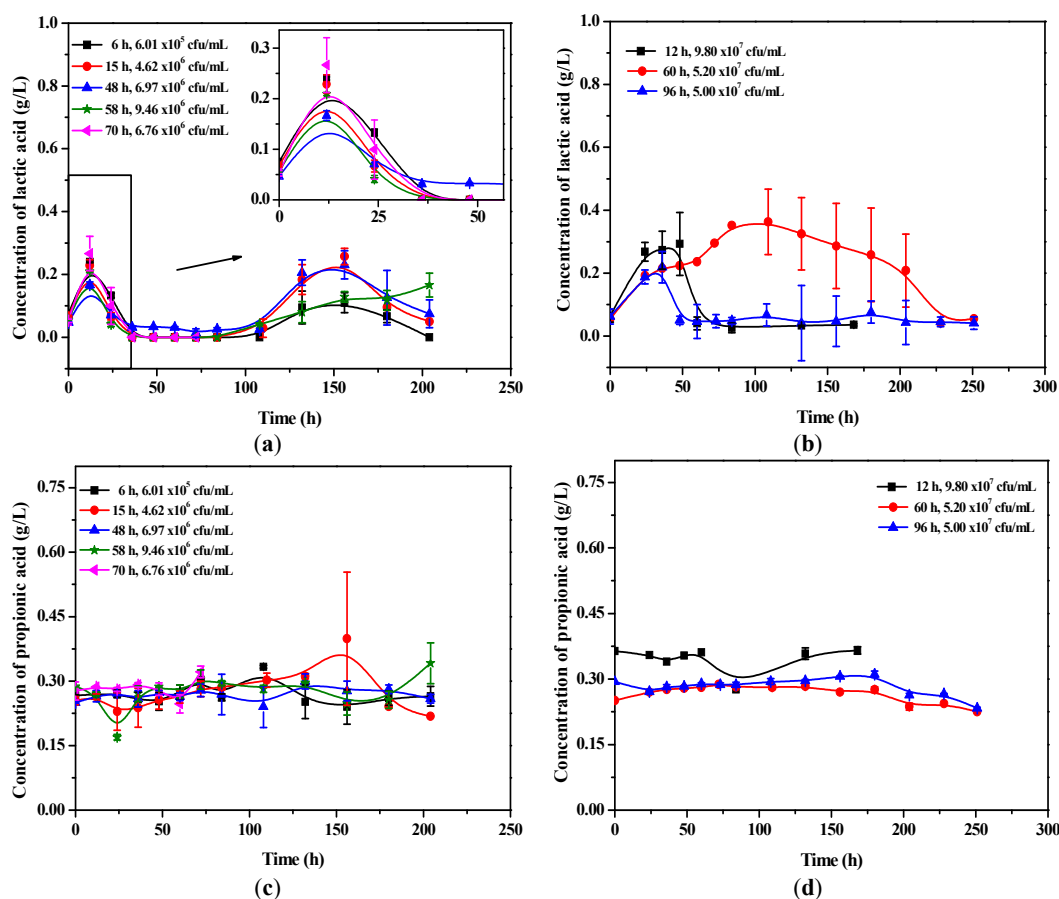


Figure 9. Time course of the concentration of lactic acid and propionic acid for *B. cereus* (a,c) and *B. naejangsansensis* (b,d) under different inoculation conditions.

As shown in Figure 9, the variation in propionic acid concentration was not significant for either strain across different inoculum ages. For *B. cereus*, the initial concentration ranged from 0.250 to 0.288 g/L at the onset of fermentation. According to Figure 4a, hydrogen production ceased after 72 h in the group with an inoculum age of 70 h, during which the propionic acid concentration exhibited an increasing trend (Figure 9c). This phenomenon may be attributed to the propionic acid synthesis pathway consuming reducing equivalents that would otherwise

be available for hydrogen production [6]. For *B. naejangsanensis* (Figure 9d), the propionic acid concentration in groups with inoculum ages of 60 h and 96 h declined gradually after a slight initial increase. However, for the group with an inoculum age of 12 h, the propionic acid concentration showed a decrease starting at 60 h, reaching its lowest level at 100 h before rising slowly until fermentation termination, coinciding with the cessation of hydrogen production. These results collectively suggest that propionic acid accumulation negatively correlates with hydrogen yield in both bacterial strains during fermentation.

Figure 10 reveals significantly different trends in formic acid concentration between the two strains. Figure 10a demonstrates that for *B. cereus*, the concentration in all five experimental groups initially increased and then decreased within 0–72 h, approaching nearly zero after 72 h. This demonstrates that *B. cereus* primarily yield hydrogen via the decomposition of formic acid, this conversion route does not suffer from inhibition in case of an increased hydrogen partial pressure since formate cleavage is an irreversible reaction as described in literature [2,21]. The initial increase likely resulted from rapid bacterial growth and metabolism fueled by nutrient-rich fermentation broth. The subsequent decrease is attributed to two factors. First is pH-driven decomposition, as shown in Figure 5a, pH declined rapidly due to organic acid accumulation within 36 h. Low pH favors the decomposition of formic acid into hydrogen, mitigating broth acidification [34]. Thus, *B. cereus* likely decomposed accumulated formic acid to counteract pH decline. Second is enzymatic conversion. Crucially, *B. cereus* converts formate to hydrogen via formate dehydrogenase [21], explaining the near-zero concentration after 72 h. Additionally, it can be further speculated that low pH may induce formate dehydrogenase expression, warranting further validation. Correlating Figures 5a and 10a, when formic acid concentration decreased at 36 h, pH values for inoculum ages of 6 h, 15 h, 48 h, 58 h and 70 h were 4.49, 4.45, 4.53, 4.45 and 4.45, respectively. This implies that enzymes like formate dehydrogenase (catalyzing H₂ and CO₂ production from formic acid) were likely be activated near pH 4.5, accelerating concentration decline. Result from Ciranna et al. [35] showed that formic acid synthesis consumes reductive ferredoxin and NADH essential for hydrogenase-mediated H₂ production, accumulated formic acid should be minimized when hydrogen as the target product. Therefore, for optimizing hydrogen yield, it is critical to prevent the formic acid accumulation during fermentation on hydrogen production.

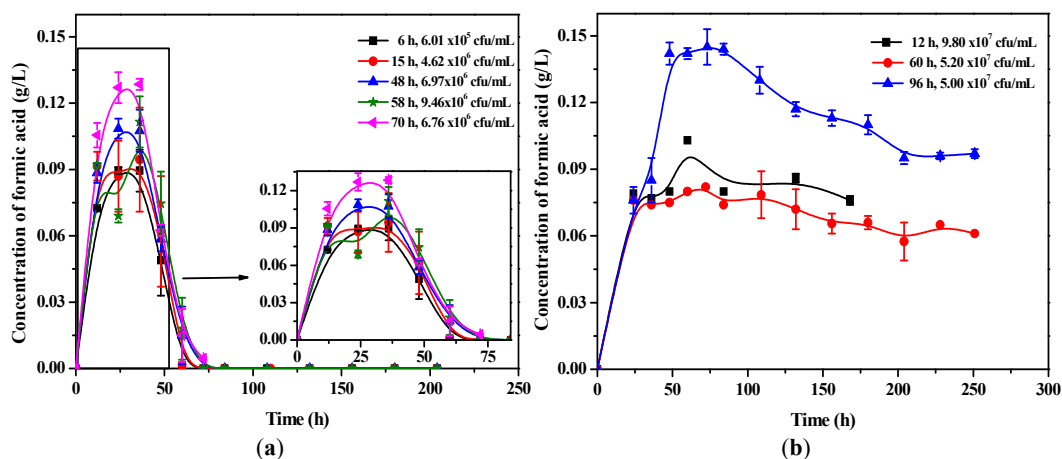


Figure 10. Time course of the concentration of formic acid for *B. cereus* (a) and *B. naejangsanensis* (b) under different inoculation conditions.

As shown in Figure 10b, for *B. naejangsanensis*, the group with an inoculum age of 96 h yielded the highest formic acid concentration (0.145 g/L at 72 h) among the three experimental groups, indicating its superior metabolic activity compared to the groups with inoculum ages of 12 h and 60 h. The formic acid production in the latter two groups remained relatively low. After reaching peak concentrations, the levels declined as fermentation progressed. According to literature [21], *B. naejangsanensis* may generate formate through amino acid catabolism when peptone serves as the sole carbon and nitrogen source. Thus, the gradual decrease in formic acid concentration across all groups likely resulted from the depletion of amino acids essential for its synthesis in the fermentation broth.

As observed from Figure 11, a large amount of butyric acid was produced during the fermentative hydrogen production process of both strains, and the acetic acid concentration was relatively higher. At the end of fermentation, for *B. cereus*, the butyric acid concentrations in the five experimental groups reached 2.185 g/L, 2.155 g/L, 2.113 g/L, 2.274 g/L and 0.836 g/L, respectively, while the corresponding acetic acid concentrations were 0.702 g/L, 0.603 g/L, 0.729 g/L, 0.610 g/L and 0.411 g/L. For *B. naejangsanensis*, the butyric acid concentrations in the three experimental

groups reached 1.348 g/L, 1.968 g/L and 1.955 g/L, respectively, with corresponding acetic acid concentrations of 0.509 g/L, 0.814 g/L and 0.96 g/L. It is evident that butyric acid and acetic acid were the dominant metabolites during the fermentative hydrogen production process for both strains under different inoculation conditions, and the sum of their concentrations exceeded 70% of the total measured metabolites. This indicates that fermentation in both strains belonged to the butyric acid-type fermentation [36–38]. From Figure 11a, it can be observed that, except for the group with an inoculum age of 48 h, the acetic acid concentration in other groups initially decreased and then increased during the early fermentation stage. This suggests that acetic acid was produced during the seed culture process for groups with inoculum ages of 6 h, 15 h, 58 h and 70 h. Based on the reported literature [21] and the composition of the seed medium, acetic acid production during the seed culture process was probably caused by the metabolism of excess amino acids, which are typically metabolized into volatile fatty acids (VFAs), such as formate, acetate, and butyrate, under anaerobic conditions. However, for the group with an inoculum age of 48 h, the metabolic pathway of *B. naejangsansensis* may have been influenced by the culture environment, resulting in no acetic acid production in the seed liquid. From the results shown in Figures 9a and 11a, it is evident that lactic acid production can influence acetic acid production during fermentative hydrogen production; this can be explained by the reported metabolic pathway of *B. cereus* [21]. Combining the result from Figure 4b with those presented in Figure 11b, cumulative H₂ production is positively correlated with the acetic acid concentration produced in the fermentative hydrogen production of *B. naejangsansensis* within a certain range. By further analyzing the results shown in Figures 4 and 11, it is found that during periods of rapid increase in acetic acid and butyric acid concentrations for both strains under different inoculum ages, cumulative H₂ production also increased correspondingly. This illustrates that changes in H₂ production during the fermentative hydrogen production process of both strains are correlated with acetic acid and butyric acid concentrations, as demonstrated by relevant research [39,40]. It's worth noting that Junghare et al. [41] also found that higher hydrogen production is correlated with acetic acid and butyric acid as fermentation products.

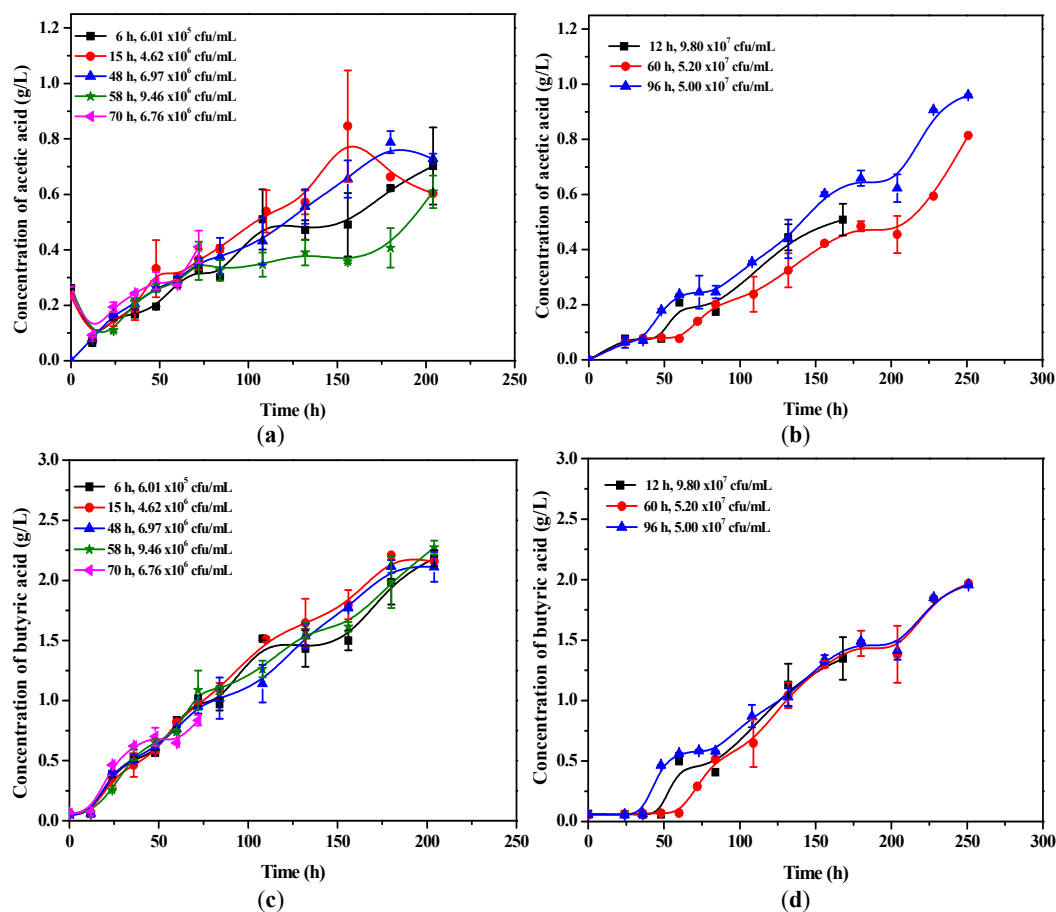


Figure 11. Time course of the concentration of acetic acid and butyric acid for *B. cereus* (a,c) and *B. naejangsansensis* (b,d) under different inoculation conditions.

3.3.7. Hydrogen Production Efficiency and Substrate Consumption Rate

According to the reported literature [1,21], in the facultative anaerobic fermentation pathway of *B. cereus*, pyruvate-converted from carbohydrates (primarily glucose) via the glycolytic pathway-is further metabolized into acetyl-CoA and formate by pyruvate formate-lyase (PFL). Subsequently, H₂ is generated from formate through the formate hydrogen-lyase enzyme complex (formate dehydrogenase). In contrast, the facultative anaerobic fermentation pathway of *B. naejangsanensis* likely involves the oxidation of pyruvate to acetyl-CoA and reduced ferredoxin (Fd) via pyruvate ferredoxin oxidoreductase (PFOR). The reduced Fd then releases H₂ through membrane-bound hydrogenase activity. Additional H₂ may be produced via NADH oxidation catalyzed by NADH-Ferredoxin reductase (NFR). Acetyl-CoA can be further metabolized into non-gaseous short-chain fatty acids (SCFAs), such as acetate, lactate, butyrate, and propionate. The theoretical maximum H₂ yield is 4 mol H₂/mol glucose for the reduced Fd pathway and 2 mol H₂/mol glucose for the formate pathway, with actual yields being influenced by concomitant fermentation end-products [42,43].

Table 2 presents the hydrogen production efficiency and substrate consumption rates of both strains under different initial inoculation conditions. The preferred inoculum age and inoculum amount for *B. cereus* were 6 h–48 h and 0.60×10^6 – 6.97×10^6 CFU/mL, respectively. The highest hydrogen production efficiency (1.93 mol H₂/mol glucose consumed) was achieved with an inoculum age of 15 h, accompanied by the maximum substrate consumption rate (62.64%). Average hydrogen production rate of this group was 8.10 mL/L/h. Notably, during the 0–100 h period, the group with an inoculum age of 15 h showed the fastest hydrogen production rate for *B. cereus* (average 11.39 mL/L/h). When using inoculum from the late deceleration growth phase (70 h), metabolic activity was prematurely inhibited by fermentation metabolites, resulting in the lowest substrate consumption rate (29.98%) at fermentation termination. These results demonstrate that *B. cereus* achieves optimal hydrogen production when inoculated during the early deceleration growth phase. For *B. naejangsanensis*, the preferred conditions were 96 h inoculum age and 5.00×10^7 CFU/mL, yielding 1.98 mol H₂/mol glucose consumed and 53.25% substrate consumption rate, with an average hydrogen production rate of 5.58 mL/L/h. The group with an inoculum age of 12 h showed premature hydrogen production termination. Although this group achieved the highest efficiency (2.19 mol H₂/mol glucose consumed), both cumulative H₂ production and substrate consumption rates were suboptimal.

Table 2. H₂ production efficiency and substrate consumption rate of both strains under different initial inoculation conditions.

Strain	Inoculum Age (h)	Inoculum Amount (CFU/mL)	Hydrogen Production Efficiency (mol H ₂ /mol Glucose Consumed)	Substrate Consumption Rate (%)
<i>B. cereus</i>	6	0.60×10^6	1.82 ± 0.07	62.63 ± 0.01
	15	4.62×10^6	1.93 ± 0.00	62.64 ± 0.00
	48	6.97×10^6	1.85 ± 0.02	59.48 ± 0.01
	58	9.46×10^6	1.76 ± 0.06	58.81 ± 0.01
	70	6.76×10^6	1.79 ± 0.07	29.98 ± 0.01
	12	9.80×10^7	2.19 ± 0.42	31.79 ± 1.73
<i>B. naejangsanensis</i>	60	5.20×10^7	1.74 ± 0.00	53.29 ± 0.00
	96	5.00×10^7	1.98 ± 0.00	53.25 ± 0.00

Notes: Under the preferred initial inoculation conditions, hydrogen yield and substrate consumption rate were measured for two H₂-producing strains: *B. cereus* (after 204 h) and *B. naejangsanensis* (after 251 h). All data were collected through batch dark fermentation.

In this study, under identical fermentation conditions and duration (204 h) except for initial inoculation parameters, the maximum H₂ yields of the two strains reached 1.93 and 2.01 mol H₂/mol glucose consumed for *B. cereus* and *B. naejangsanensis*, respectively, representing 96.50% and 50.25% of their theoretical maxima. When comparing the H₂ production efficiency under preferred initial inoculation conditions with the results reported in the literature [5], both strains showed significant improvements, *B. cereus* achieved 3.8-fold enhancement, while *B. naejangsanensis* exhibited 4.5-fold increase. Although *B. cereus* demonstrated superior starch-hydrolyzing capacity according to previous reports [21], its final H₂ yield in monoculture fermentation was lower than *B. naejangsanensis*, suggesting higher metabolic efficiency in the latter strain. However, comprehensive evaluation incorporating both H₂ yield and substrate utilization revealed *B. cereus* as the more effective producer. After 204 h fermentation, *B. cereus* maintained a substantially higher substrate consumption rate (62.64%) compared to *B. naejangsanensis* (39.18%), indicating better overall process efficiency.

Hydrogen yields obtained from single fermentation under the preferred initial inoculation conditions in this study (1.93 mol H₂/mol glucose consumed for *B. cereus* and 1.98 mol H₂/mol glucose consumed for *B. naejangsanensis*) exceeded those reported by Bao et al. [5] and Wang et al. [18,44] for mixed-culture systems. Specifically, Bao et al. [5] achieved 1.04 mol H₂/mol glucose, while Wang et al. [18,44] reported 1.72 and 1.88 mol H₂/mol glucose, respectively. Additionally, the mixed-culture hydrogen yield of 1.94 mol H₂/mol glucose consumed from Bao et al. [17] closely matched the *B. cereus* yield in this study. Discrepancies in hydrogen yields arise from microbial strain differences, culture conditions, fermentation mode (batch vs. continuous), and substrate types and so on [45]. Overall, single-strain fermentation under the preferred initial inoculation conditions in this study demonstrated superior hydrogen yields compared to both published single-strain and mixed-culture results.

4. Conclusions

Initial inoculation conditions for hydrogen production in *Bacillus cereus* and *B. naejangsanensis* monocultures were optimized in batch mode. The preferred initial inoculation conditions of both strains were obtained. For *B. cereus*, the preferred inoculum age was 15 h (inoculum amount: 4.62×10^6 CFU/mL), achieving a maximum hydrogen yield of 1.93 mol H₂/mol glucose consumed with 62.64% substrate consumption rate after 204 h. For *B. naejangsanensis*, optimal conditions were 96 h inoculum age (5.00×10^7 CFU/mL), yielding 1.98 mol H₂/mol glucose consumed and 53.25% substrate utilization after 251 h. Hydrogen production correlated directly with cellular growth in both strains. Results also showed that *B. cereus* exhibited maximal starch utilization efficiency when inoculated during the early deceleration growth phase, while *B. naejangsanensis* performed optimally in the late deceleration growth phase. Starch hydrolysis to soluble sugars occurred 24 h faster in *B. cereus* than *B. naejangsanensis*. Metabolic analysis revealed that when metabolic pathway shifted to produce lactic and propionic acid, hydrogen production decreased, elevated acetic and butyric acid concentrations correlated with higher hydrogen production. Butyric-type fermentation dominated metabolic pathways in both strains. Integrating H₂ yield, substrate consumption rate and characteristics of yielding hydrogen route, *B. cereus* demonstrated superior performance for starch-based hydrogen production. These findings provide fundamental data for scaling-up coculture fermentative system and its continuous operation. Subsequently, effect of pH on formate dehydrogenase activity should be proved. Additionally, in order to clearly understand the metabolic mechanisms of both H₂-producing strains, further improve their substrate utilization efficiency and environmental robustness for complex fermentation systems, the following strategies should be implemented in the future work: (1) genetic-level metabolic engineering to upregulate formate dehydrogenase and hydrogenase expression while modifying associated metabolic pathways; (2) quantitative profiling of energy carriers (NAD⁺/NADH₂, Fd_{ox}/Fd_{red} and ATP/ADP ratios); (3) development of novel bioreactors with specialized structural and functional designs.

Author Contributions

H.M.: design and perform experiment, data treatment, writing—original draft, writing—review & editing; Q.K.: Modified the manuscript and provided some valuable suggestions. All authors have read and agreed to the published version of the manuscript.

Funding

The authors would like to express their gratitude to the Research Project (2003/205040322) of Yan'an University.

Data Availability Statement

Data will be made available on request.

Acknowledgments

The authors thank the School of Life Science and Technology of the Beijing University of Technology for granting support to perform experiments in its laboratories.

Conflicts of Interest

The authors declare that they have no competing interests.

References

1. Dzul'karnain, E.L.N.; Audu, J.O.; Wan Dagang, W.R.Z.; et al. Microbiomes of biohydrogen production from dark fermentation of industrial wastes: Current trends, advanced tools and future outlook. *Bioresour. Bioprocess.* **2022**, *9*, 16. <https://doi.org/10.1186/s40643-022-00504-8>.
2. Baeyens, J.; Zhang, H.L.; Nie, J.P.; et al. Reviewing the potential of bio-hydrogen production by fermentation. *Renew. Sustain. Energy Rev.* **2020**, *131*, 110023. <https://doi.org/10.1016/j.rser.2020.110023>.
3. Dahiya, S.; Chatterjee, S.; Sarkar, O.; et al. Renewable hydrogen production by dark-fermentation: Current status, challenges and perspectives. *Bioresour. Technol.* **2021**, *321*, 124354. <https://doi.org/10.1016/j.biortech.2020.124354>.
4. Rahman, S.N.A.; Masdar, M.S.; Rosli, M.I.; et al. Overview biohydrogen technologies and application in fuel cell technology. *Renew. Sustain. Energy Rev.* **2016**, *66*, 137–162.
5. Bao, M.D.; Su, H.J.; Tan, T.W. Biohydrogen production by dark fermentation of starch using mixed bacterial cultures of *Bacillus* sp. and *Brevumdimonas* sp. *Energy Fuels* **2012**, *26*, 5872–5878. <https://doi.org/10.1021/ef300666m>.
6. Lee, H.S.; Krajmalinik-Brown, R.; Zhang, H.; et al. An electron-flow model can predict complex redox reactions in mixed-culture fermentative BioH₂: Microbial ecology evidence. *Biotechnol. Bioeng.* **2009**, *104*, 687–697. <https://doi.org/10.1002/bit.22442>.
7. Li, Y.F.; Ren, N.Q.; Chen, Y.; et al. Ecological mechanism of fermentative hydrogen production by bacteria. *Int. J. Hydrogen Energy* **2007**, *32*, 755–760. <https://doi.org/10.1016/j.ijhydene.2006.08.004>.
8. Hawkes, F.R.; Hussy, I.; Kyazze, G.; et al. Continuous dark fermentative hydrogen production by mesophilic microflora: Principles and progress. *Int. J. Hydrogen Energy* **2007**, *32*, 172–184. <https://doi.org/10.1016/j.ijhydene.2006.08.014>.
9. Levin, D.B.; Islam, R.; Cicek, N.; et al. Hydrogen production by *Clostridium thermocellum* 27405 from cellulosic biomass substrates. *Int. J. Hydrogen Energy* **2006**, *31*, 1496–1503. <https://doi.org/10.1016/j.ijhydene.2006.06.015>.
10. Yokoi, H.; Tokushige, T.; Hirose, J.; et al. Hydrogen production by immobilized cells of aciduric *Enterobacter aerogenes* strain HO-39. *J. Ferment. Bioeng.* **1997**, *83*, 481–484. [https://doi.org/10.1016/S0922-338X\(97\)83006-1](https://doi.org/10.1016/S0922-338X(97)83006-1).
11. Du, J.; Zhou, J.; Xue, J.; et al. Metabolomic profiling elucidates community dynamics of the *Ketogulonicigenium vulgare-Bacillus megaterium* consortium. *Metabolomics* **2012**, *8*, 960–973. <https://doi.org/10.1007/s11306-011-0392-2>.
12. Wang, X.Y.; Jin, B. Process optimization of biological hydrogen production from molasses by a newly isolated *Clostridium butyricum* W5. *J. Biosci. Bioeng.* **2009**, *107*, 138–144. <https://doi.org/10.1016/j.jbiosc.2008.10.012>.
13. Azman, N.F.; Abdeshahian, P.; Kadier, A.; et al. Utilization of palm kernel cake as a renewable feedstock for fermentative hydrogen production. *Renew. Energy* **2016**, *93*, 700–708. <https://doi.org/10.1016/j.renene.2016.03.046>.
14. Li, Q.; Liu, C.Z. Co-culture of *Clostridium thermocellum* and *Clostridium thermosaccharolyticum* for enhancing hydrogen production via thermophilic fermentation of cornstalk waste. *Int. J. Hydrogen Energy* **2012**, *37*, 10648–10654. <https://doi.org/10.1016/j.ijhydene.2012.04.115>.
15. Ma, H.X.; Su, H.J. Effect of temperature on the fermentation of starch by two high efficient H₂ producers. *Renew. Energy* **2019**, *138*, 964–970. <https://doi.org/10.1016/j.renene.2019.01.126>.
16. Ma, H.X.; Liu, Y.; Li, Z.P. The synergistic hydrogen production of bicellular fermentation systems and fluid dynamics simulation in reactor under stirring. *Bioresour. Technol. Rep.* **2023**, *22*, 101473. <https://doi.org/10.1016/j.biteb.2023.101473>.
17. Bao, M.D.; Su, H.J.; Tan, T.W. Dark fermentative bio-hydrogen production: Effects of substrate pre-treatment and addition of metal ions or L-cysteine. *Fuel* **2013**, *112*, 38–44. <https://doi.org/10.1016/j.fuel.2013.04.063>.
18. Wang, S.J.; Ma, Z.H.; Zhang, T.; et al. Optimization and modeling of biohydrogen production by mixed bacterial cultures from raw cassava starch. *Front. Chem. Sci. Eng.* **2017**, *11*, 100–106. <https://doi.org/10.1007/s11705-017-1617-3>.
19. Miller, G.L. Use of dinitrosalicylic acid reagent for determination of reducing sugars. *Anal. Chem.* **1959**, *31*, 426–428. <https://doi.org/10.1021/ac60147a030>.
20. Abdeshahian, P.; Al-Shorgani, N.K.N.; Salih, N.K.M.; et al. The production of biohydrogen by a novel strain *Clostridium* sp. YM1 in dark fermentation process. *Int. J. Hydrogen Energy* **2014**, *39*, 12524–12531. <https://doi.org/10.1016/j.ijhydene.2014.05.081>.
21. Wang, S.J.; Tang, H.Z.; Peng, F.; et al. Metabolite-based mutualism enhances hydrogen production in a two-species microbial consortium. *Commun. Biol.* **2019**, *2*, 82. <https://doi.org/10.1038/s42003-019-0331-8>.
22. Liu, I.C.; Whang, L.M.; Ren, W.J.; et al. The effect of pH on the production of biohydrogen by clostridia: Thermodynamic and metabolic considerations. *Int. J. Hydrogen Energy* **2011**, *36*, 439–449. <https://doi.org/10.1016/j.ijhydene.2010.10.045>.
23. Dada, O.; Yusoff, W.M.W.; Kalil, M.S. Biohydrogen production from ricebran using *Clostridium saccharoperbutylacetonicum* N1-4. *Int. J. Hydrogen Energy* **2013**, *38*, 15063–15073. <https://doi.org/10.1016/j.ijhydene.2013.07.048>.
24. Li, W.M.; Cheng, C.; Ren, N.Q.; et al. Different feedback effects of aqueous end products on hydrogen production of *Clostridium tyrobutyricum*. *Int. J. Hydrogen Energy* **2022**, *47*, 35156–35170. <https://doi.org/10.1016/j.ijhydene.2022.08.120>.
25. Vassilev, I.; Gießelmann, G.; Schwechheimer, S.K.; et al. Anodic electro-fermentation: Anaerobic production of L-Lysine by recombinant *Corynebacterium glutamicum*. *Biotechnol. Bioeng.* **2018**, *115*, 1499–1508. <https://doi.org/10.1002/bit.26562>.

26. Rasdi, Z.; Mumtaz, T.; Rahman, N.A.A.; et al. Kinetic analysis of biohydrogen production from anaerobically treated POME in bioreactor under optimized condition. *Int. J. Hydrogen Energy* **2012**, *37*, 17724–17730. <https://doi.org/10.1016/j.ijhydene.2012.08.095>.
27. Khanal, S.K.; Chen, W.H.; Li, L.; et al. Biological hydrogen production: Effects of pH and intermediate products. *Int. J. Hydrogen Energy* **2004**, *29*, 1123–1131. <https://doi.org/10.1016/j.ijhydene.2003.11.002>.
28. Chin, H.L.; Chen, Z.S.; Chou, C.P. Fedbatch operation using *Clostridium acetobutylicum* suspension culture as biocatalyst for enhancing hydrogen production. *Biotechnol. Prog.* **2003**, *19*, 383–388. <https://doi.org/10.1021/bp0200604>.
29. Ergal, İ.; Fuchs, W.; Hasibar, B.; et al. The physiology and biotechnology of dark fermentative biohydrogen production. *Biotechnol. Adv.* **2018**, *36*, 2165–2186. <https://doi.org/10.1016/j.biotechadv.2018.10.005>.
30. Verhaart, M.R.A.; Bielen, A.A.M.; Van der Oost, J.; et al. Hydrogen production by hyperthermophilic and extremely thermophilic bacteria and archaea: Mechanisms for reductant disposal. *Environ. Technol.* **2010**, *31*, 993–1003. <https://doi.org/10.1080/09593331003710244>.
31. Chittibabu, G.; Nath, K.; Das, D. Feasibility studies on the fermentative hydrogen production by recombinant *Escherichia coli* BL-21. *Process Biochem.* **2006**, *41*, 682–688. <https://doi.org/10.1016/j.procbio.2005.08.020>.
32. Willquist, K.; van Niel, E.W.J. Lactate formation in *Caldicellulosiruptor saccharolyticus* is regulated by the energy carriers pyrophosphate and ATP. *Metab. Eng.* **2010**, *12*, 282–290. <https://doi.org/10.1016/j.ymben.2010.01.001>.
33. Antonopoulou, G.; Gavala, H.N.; Skiadas, I.V.; et al. Influence of pH on fermentative hydrogen production from sweet sorghum extract. *Int. J. Hydrogen Energy* **2010**, *35*, 1921–1928. <https://doi.org/10.1016/j.ijhydene.2009.12.175>.
34. Hallenbeck, P.C. Fermentative hydrogen production: Principles, progress, and prognosis. *Int. J. Hydrogen Energy* **2009**, *34*, 7379–7389. <https://doi.org/10.1016/j.ijhydene.2008.12.080>.
35. Ciranna, A.; Ferrari, R.; Santala, V.; et al. Inhibitory effects of substrate and soluble end products on biohydrogen production of the alkalithermophile *Caloramator celer*: Kinetic, metabolic and transcription analyses. *Int. J. Hydrogen Energy* **2014**, *39*, 6391–6401. <https://doi.org/10.1016/j.ijhydene.2014.02.047>.
36. Nicolaou, S.A.; Gaida, S.M.; Papoutsakis, E.T. A comparative view of metabolite and substrate stress and tolerance in microbial bioprocessing: From biofuels and chemicals, to biocatalysis and bioremediation. *Metab. Eng.* **2010**, *12*, 307–331. <https://doi.org/10.1016/j.ymben.2010.03.004>.
37. Li, W.M.; He, L.; Cheng, C.; et al. Effects of biochar on ethanol-type and butyrate-type fermentative hydrogen productions. *Bioresour. Technol.* **2020**, *306*, 123088. <https://doi.org/10.1016/j.biortech.2020.123088>.
38. Li, S.; Kang, Q.; Baeyens, J.; et al. Hydrogen production: State of technology. *IOP Conf. Ser. Earth Environ. Sci.* **2020**, *544*, 012011. <https://doi.org/10.1088/1755-1315/544/1/012011>.
39. Zhao, M.X.; Ruan, W.Q. Improving hydrogen generation from kitchen wastes by microbial acetate tolerance response. *Energ. Convers. Manag.* **2014**, *77*, 419–423. <https://doi.org/10.1016/j.enconman.2013.10.007>.
40. Cotter, P.D.; Hill, C. Surviving the acid test: Responses of gram-positive bacteria to low pH. *Microbiol. Mol. Biol. Rev.* **2003**, *67*, 429–453. <https://doi.org/10.1128/MMBR.67.3.429-453.2003>.
41. Junghare, M.; Subudhi, S.; Lal, B. Improvement of hydrogen production under decreased partial pressure by newly isolated alkaline tolerant anaerobe, *Clostridium butyricum* TM-9A: Optimization of process parameters. *Int. J. Hydrogen Energy* **2012**, *37*, 3160–3168. <https://doi.org/10.1016/j.ijhydene.2011.11.043>.
42. Keskin, T.; Abubakar, H.N.; Yazgin, O.; et al. Effect of percolation frequency on biohydrogen production from fruit and vegetable wastes by dry fermentation. *Int. J. Hydrogen Energy* **2019**, *44*, 18767–18775. <https://doi.org/10.1016/j.ijhydene.2018.12.099>.
43. Vardar-Schara, G.; Maeda, T.; Wood, T.K. Metabolically engineered bacteria for producing hydrogen via fermentation. *Microb. Biotechnol.* **2008**, *1*, 107–125. <https://doi.org/10.1111/j.1751-7915.2007.00009.x>.
44. Wang, S.J.; Zhang, T.; Su, H.J. Enhanced hydrogen production from corn starch wastewater as nitrogen source by mixed cultures. *Renew. Energy* **2016**, *96*, 1135–1141. <https://doi.org/10.1016/j.renene.2015.11.072>.
45. Elsharnouby, O.; Hafez, H.; Nakhla, G.; et al. A critical literature review on biohydrogen production by pure cultures. *Int. J. Hydrogen Energy* **2013**, *38*, 4945–4966. <https://doi.org/10.1016/j.ijhydene.2013.02.032>.